Subsurface Evidence of Storm-Driven Breaching along a Transgressing Barrier System, Cape Cod, U.S.A.

Christopher V. Maio[†][*], **Allen M. Gontz**[‡], **Richard M. Sullivan**[§], **Stephanie M. Madsen**[§], **Christopher R. Weidman**[††], **and Jeffrey P. Donnelly**[§]

[†]Department of Geosciences
University of Alaska Fairbanks
Fairbanks, AK 99775, U.S.A.

[‡]School for the Environment
University of Massachusetts–Boston
Boston, MA 02125, U.S.A.

[§]Coastal Systems Group
Woods Hole Oceanographic
   Institution
Woods Hole, MA 02543, U.S.A.

[††]Waquoit Bay National Estuarine Research Reserve
Waquoit, MA 02536, U.S.A.

www.cerf-jcr.org

www.JCRonline.org

ABSTRACT

Maio, C.V.; Gontz, A.M.; Sullivan, R.M.; Madsen, S.M.; Weidman, C.R., and Donnelly, J.P., 0000. Subsurface evidence of storm-driven breaching along a transgressing barrier system, Cape Cod, U.S.A. *Journal of Coastal Research,* 00(0), 000–000. Coconut Creek (Florida), ISSN 0749-0208.

Relict and historic tidal channels buried within coastal barriers provide a geologic signature of environmental change, thus enhancing our understanding of how barrier systems respond to extreme storm events. Earliest maps from 1846 depict three inlets along the Waquoit Bay barrier system located on Cape Cod, Massachusetts. These channels were not depicted on maps after 1846, and we lack any information pertaining to them before 1846. The principle objective of this study was to identify the location and map the internal geometry and channel-fill configuration of the buried inlet structures using geophysical and sedimentological data acquisition methods. This was done by collecting 6.2 km of shore-parallel ground-penetrating radar data and five sediment cores ranging in depth from 4 to 5 m. The sediment cores allowed for the ground truthing of the ground-penetrating radar data and provided six samples for radiocarbon dating. The 13 paleochannels identified ranged in depths from 1.3 to 3.7 m below the present beach surface. These appeared in the radar imagery as broad U-shaped cut-and-fill features incised into adjacent barrier facies. The 13 paleochannels composed 24% of the barrier lithosome totaling 704 m in length. Individual channels were primarily less than 65 m in length and between 2.5 and 1.3 m in depth, although an additional 275-m-wide, 3.7-m-deep channel sequence was imaged and likely represents a major and long-lived paleochannel. The results will contribute toward deciphering the evolution of the Waquoit system and identify areas vulnerable to storm-driven coastal change.

ADDITIONAL INDEX WORDS: *Coastal evolution, marine transgression, ground-penetrating radar, overwash, South Cape Beach, paleochannel, paleogeography, coastal change.*

INTRODUCTION

Baymouth barrier systems are critical components to coastal environments, yielding numerous benefits to human society (Ashton, Donnelly, and Evans, 2008; FitzGerald *et al.*, 2008; Nicholls *et al.*, 2007; van Heteren *et al.*, 1998). These benefits include the formation of back-barrier lagoons that provide abundant ecosystem services (Barbier, 2012; Salzman, 1997). They allow for the development of safe harbors (Turner *et al.*, 1998), nursery grounds for commercially important fish species, and areas for recreation (Barbier *et al.*, 2011). In New England, most coastal barriers were formed during the past 5000 years and derived their sediments from the transgressive reworking of glacial and fluvial deposits (Belknap, Gontz, and Kelley, 2005; FitzGerald, Buynevich, and Rosen, 2001; Uchupi and Mulligan, 2006; van Heteren *et al.*, 1998). The continued rise in sea level coupled with a coeval reduction in sediment supply make retrograding barriers a relatively common landform along the formally glaciated coastline of Massachusetts (FitzGerald, Buynevich, and Rosen, 2001; Gutierrez *et al.*, 2003).

Relict tidal inlets buried within the beach lithosome provide a geologic signature of past environmental change, including the location and geometry of the past breaches and a record of back-barrier hydrodynamics (FitzGerald, Buynevich, and Rosen, 2001; Hein *et al.*, 2012; Seminack and Buynevich, 2013). The identification of former paleochannels is important because such identification extends the record of barrier breaching, which in turn aids our understanding of coastal processes and barrier responses to extreme storm events (Buynevich and FitzGerald, 2003; Mallinson *et al.*, 2010).

The dynamic barrier system is a vulnerable landform and ecosystem susceptible to storm-driven morphological modification (Donnelly *et al.*, 2004). A barrier may be breached when powerful storm surges and waves cut through a portion of the shoreface (Buynevich, FitzGerald, and van Heteren, 2004; FitzGerald, van Heteren, and Montello, 1994), allowing for marine waters to episodically flood into the back-barrier environment. The resulting breachway may persist long after the storm has passed or infill rapidly, depending on the extent of the original breach and the coastal processes at work in the region. One of the major coastal processes in regards to inlet dynamics is longshore sediment transport, which often leads to channel migration and filling (Hayes, 1980). Regardless of the longevity of these breaches, once infilled, their sedimentary signatures are archived in the barrier lithosomes and are
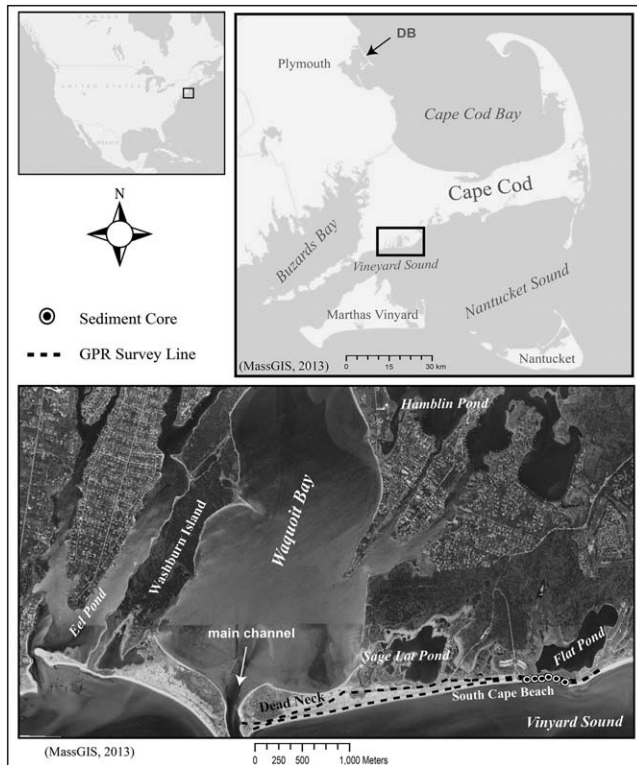
Figure 1. Grayscale base map of study site located along the Waquoit barrier system on Cape Cod, Massachusetts, U.S.A. (MassGIS, 2013). The black dashed line shown on a MassGIS 2008 orthophotograph marks the GPR survey transect totaling 6.2 km. Sediment core locations are also identified with small round bull's-eyes. Duxbury Beach (DB) is identified as the location of previous research (FitzGerald, Buynevich, and Rosen, 2001; MassGIS, 2013).

diagnostic of a transgressive system (FitzGerald, Buynevich, and Rosen, 2001; Seminack and Buynevich, 2013; van Heteren *et al.,* 1998).

Storm-driven barrier breaching and the formation of new inlets can lead to dramatic perturbations in adjacent coastal landforms and ecosystems (Buynevich and FitzGerald, 2003; Mallinson *et al.*, 2011). These include a potential rapid increase in wave and tidal energy within back-barrier settings, the salinization of freshwater environments, alterations to important marine transportation routes, and the destruction of coastal infrastructure (Buynevich and FitzGerald, 2003; FitzGerald, van Heteren, and Montello, 1994; Maio *et al.*, 2014; Mallinson *et al.*, 2011). Because of these factors, developing a long-term understanding of barrier inlet dynamics and susceptibility to breaching events is a critical topic to be addressed and is a major concern for coastal managers and engineers (FitzGerald *et al.*, 2008; Khalil, Finkl, and Raynie, 2013; Seminack and Buynevich, 2013).

Until recently, existing knowledge on former channel locations and barrier evolution was primarily based on historical maps, extensive core and trench efforts, and surficial geomorphic observations (Buynevich, 2003; Jol, Smith, and

Meyers, 1996; van Heteren *et al.*, 1998). Since 1990, the use of ground-penetrating radar (GPR) to identify the location of buried paleochannels has steadily grown (Buynevich, 2003; FitzGerald, Buynevich, and Rosen, 2001; FitzGerald and van Heteren, 1999; Mallinson *et al.*, 2010). Similar studies in Massachusetts along Duxbury Beach, Plymouth, identified a minimum of 18 historic and prehistoric paleochannels. The channel structures made up more than 25% of the total barrier lithosome, with lengths ranging between 27 and 200 m and depths between 1.3 and 4 m (FitzGerald, Buynevich, and Rosen, 2001). Such a study demonstrates not only the wealth of information archived in the sand relating to back-barrier hydrodynamics, but also the viability of GPR as a method to access this record.

The purpose of this study is to identify the major radar and lithofacies and determine the location and extent of relict inlets buried within the Waquoit barrier lithosome. This information will provide important data sets that contribute toward understanding the paleoenvironmental evolution of the Waquoit barrier system. This will be achieved through three primary objectives: (1) delineate radar and lithofacies based on GPR and core data, (2) identify buried paleochannel structures and assess the geometry of preclosure inlet cross sections and channel-fill patterns, and (3) develop age control for the formation and closing of relict and historic inlets. The research will contribute to the broader spatial and temporal understanding of the coastal paleoenvironmental evolution of the barrier system.

Study Site

The study site is located along the Waquoit barrier system on the south shore of Cape Cod, Massachusetts, approximately 90 km southeast of Boston, centered at 41.5514° N latitude and 70.5110° W longitude (Figure 1). This shallow water lagoon reaches a maximum depth of 3 m and encompasses an area of 3.7 km^2, with a mean tidal fluctuation of approximately 0.79 m. Average wave height within the Vineyard Sound is approximately 0.6 m, with higher waves occurring during high-energy storm events. Hurricane-driven storm tides as high as 2.5 m above mean high high water have been recorded at the nearby National Oceanic and Atmospheric Administration (NOAA)–operated Woods Hole tide gauge (NOAA, 2014). The geologic framework of the Waquoit barrier consists of reworked paraglacial sediments. During the end of the Wisconsin Glacial, the Laurentide Ice Sheet reached its southern terminus at Nantucket and Martha's Vineyard islands approximately 23,000 YBP (Balco *et al.,* 2002). The relict glacial topography has been subsequently altered by fluvial, coastal, and aeolian processes and provides the geologic framework for the Waquoit system (Gutierrez *et al.,* 2003; Oldale and O'Hara, 1984; Uchupi and Mulligan, 2006).

The present baymouth barrier is 2.9 km in length trending along an east-west axis and separates Waquoit Bay on its northern side from the Vineyard Sound to the south. The western end of the barrier, known as Dead Neck, terminates at the navigable entrance to Waquoit Bay. The main channel was stabilized with jetties in 1930 (Keay, 2001) and continues to be maintained as a navigable waterway. Based on an 1846 U.S. Navy Coast Survey (Coast Survey) map (Boston Survey
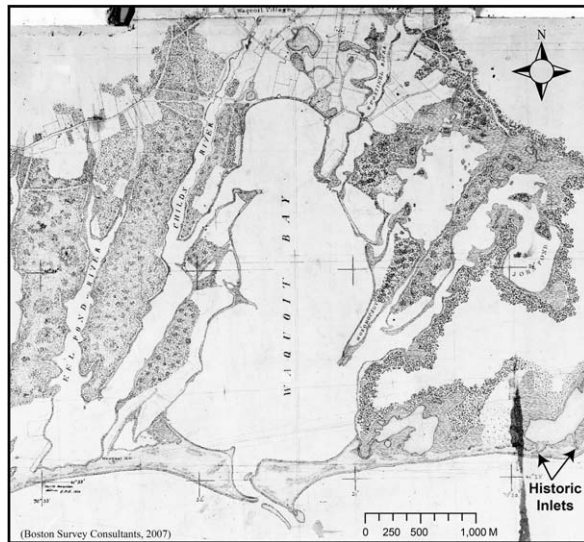
Figure 2. Spatially referenced 1846 U.S. Navy Coast Survey map of the Waquoit system (Boston Survey Consultants, 2007). The map represents the earliest and most accurate representation of the historic shoreline. Three historic inlets and a flood tide delta are identified with the black arrow along the eastern portion of the barrier fronting Flat Pond. These former inlets are located above the delineated high water line, likely indicating they were becoming less active by this point in time. The inlets do not appear on later maps or presently exist.

Consultants, 2007) the prestabilized channel was approximately 150 m wide at its center, whereas the present channel has a width of 100 m at its center (Figure 2). Presently the channel is between 4 and 5 m in depth. Although no information exists on the channel's prestabilization depth, based on its larger width during historic times it likely was shallower, at a depth between 2 and 4 m (MassGIS, 2013). Washburn Island extends the barrier westward from the main channel. To the east of the channel, the barrier protects an extensive salt marsh system, which joins two salt ponds, Sage Lot Pond and Flat Pond. This portion of the barrier, referred to as South Cape Beach, is very narrow, with some areas less than 50 m wide. The far eastern end of the barrier is welded to uplands and has been heavily modified through private development. The Coast Survey map shows that there were three former inlets connecting Flat Pond to Vineyard Sound; yet, no inlets exist today (Boston Survey Consultants, 2007) (Figure 2).

METHODS

To achieve our research objectives GPR and percussion coring will be used. The GPR allows for a more targeted site selection before coring. The radar data reveal the location of buried paleochannels while also recording their geometry and offering insight into the nature of channel infilling. From this data, coring locations can be chosen that maximize the recovery of the channel-fill sequence and offer a more complete inlet record from which the site evolution can be inferred. GPR can be used to define broader features,

whereas sediment coring gives high-resolution *in situ* data at point locations. Cores also help ground truth key bounding surfaces and radar facies and obtain samples for textural analysis and chronological control.

Ground-Penetrating Radar

GPR is a noninvasive method that utilizes electromagnetic (EM) waves to probe the Earth's subsurface (Neal and Roberts, 2000) and provides a rapid and inexpensive means of identifying subsurface geologic features and stratigraphic relationships to long-term geomorphic trends (FitzGerald, Buynevich, and Rosen, 2001; Gontz *et al.*, 2011; Hein *et al.*, 2012; Neal and Roberts, 2000; Seminack and Buynevich, 2013; van Heteren *et al.*, 1998). More than 6.2 km of GPR data were collected using a MALÅ Geosciences ProEx Control Unit coupled with a 500-MHz antenna. Reconnaissance level surveys were also carried out using a 100-MHz antenna, although because of attenuation of the signal, this did not increase penetration and resulted in lower resolution data. Therefore, the 500-MHz data were used in this study. GPR data were collected in a continuous recording mode with a sampling rate of 10 Hz. Penetration varied between 150 and 250 ns, with various gains selected during the collection of data to optimize the displayed output. Position information came from a Garmin 76Csx GPS with a log frequency of 0.1 seconds (also 10Hz). The GPR was towed from either an all-terrain vehicle or pulled by hand along beach and sand access trails. Topographic corrections were not necessary because of minimal elevation changes encountered along shore-parallel transects, especially in areas that paleochannel facies were identified (FitzGerald, Buynevich, and Rosen, 2001). A collection speed between 0.9 and 1.34 m/s was maintained throughout the survey.

Resolutions vary based on penetrative depth and the properties of the sediments. Horizontal resolution refers to the smallest along-track size of an object that can be imaged by the radar (Neal, 2004). Based on the methods presented by Neal (2004), the horizontal resolution of the Waquoit barrier surveys was calculated to be 61 cm through wet sands at a depth of 1 m. The vertical resolution refers to the required thickness of an object in the *z* direction before it can be resolved by GPR. Typically the resolving power is thought to be between one quarter to a half the wavelength of the EM signal through the subsurface (Neal and Roberts, 2000; Neal 2004). Based on the formulas outlined by Neal (2004) and the use of the 500-MHz antenna in saturated sand, we calculated a vertical resolution of approximately 15–20 cm.

GPR data was postprocessed using RadExplorer v. 1.4. Data were minimally processed, applying four RadExplorer routines and the default settings. These processing routines included, DC removal, background removal, amplitude correction (gain), and band-pass filtering. The mixed nature of the sediment types along the Waquoit barrier possesses the lithological heterogeneity necessary for resolving the facies boundaries in the radar images. On the basis of core data and previous research (*i.e.*, Gontz *et al.*, 2011; Mallinson *et al.*, 2010; van Heteren *et al.*, 1996), we applied a 0.067 m/ns EM velocity to calculate the approximate depth of radar reflectors, which assumes the sediments are saturated below the surface and therefore do not warrant a two-layer model.

Sediment Cores

Five sediment cores (SCB1–SCB5) were obtained using a Geoprobe Systems model TR54 mounted on a 4115 John Deere tractor. Core sites were situated along the backshore between the high water line (HWL) and foredune areas. The Geoprobe collects cores in 5-cm-diam clear polycarbonate tubes in 1-m consecutive sections. The maximal coring depth was determined by the GPR data and a visual onsite interpretation of the cores as they were recovered. After recovery the cores were returned to the Woods Hole Oceanographic Institution's Coastal Research Laboratory, where they were stored at 4°C. Sediment core analysis consisted of splitting, photographing, and describing the cores by sediment type, texture, character of the transitions between horizons, and color. Two additional Geoprobe cores (WB1 and WB2) were collected at the same location in 2011 (Maio *et al.*, 2014) and have been incorporated into the analysis.

Correlating subsurface features located in GPR imagery with those identified *in situ* through sediment cores is inherently uncertain. EM propagation speeds vary through material transitions because the dielectric constant is not uniform from one sediment type to another (dry sand vs. wet clay vs. peat). Although detailed postprocessing can refine the propagation speeds (and thus the speed/depth conversion), the degree of accuracy to which this can be done is not absolute. Further complicating such geophysical/sedimentological correlations is the issue of compaction. The Geoprobe Coring system utilizes a hydraulic hammer to drive the sample barrels into the subsurface. The force required by this will compact softer sediment layers, skewing the depths of these layers downward. Compaction was not a major issue within the cores because they predominately consisted of sand, with only small horizons of the more compressible peat. Although sampling techniques do exist that minimize this issue, they are either highly invasive (trenching) or insufficient in power to penetrate sands to any meaningful depth (hand-driven percussion coring, vibracoring, or Russian peat coring).

Radiocarbon Dating

Radiocarbon samples were identified and collected from the SCB4, SCB5, and WB2 (Maio *et al.*, 2014) sediment cores and submitted to the National Ocean Sciences Accelerator Mass Spectrometry (NOSAMS) facility at the Woods Hole Oceanographic Institution for accelerator mass spectrometry (AMS) radiocarbon dating and isotopic carbon analysis. All samples were processed according to NOSAMS specifications (NOSAMS, 2014). In addition to the traditional AMS method, NOSAMS also has developed a 500-kV Pelletron-based AMS system with a novel gas-accepting ion-source that was employed for dating carbonate shell samples. This new continuous-flow AMS (CFAMS) method is capable of analyzing CO_2 gas directly and, hence, skips conversion to the graphite process (Roberts *et al.*, 2013). We employed traditional AMS methods to determine the age of plant matter sampled from the cores, whereas carbonate shells were dated using CFAMS.

All organic-derived AMS ages and carbonate shell-derived CFAMS ages were calibrated using Calib v. 7.0.1 with the IntCal13 and Marine13 calibration data sets, respectively (Reimer *et al.*, 2009). A regional reservoir correction of $\Delta R = -95$

$\pm\ 45\ ^{14}$C years (Little, 1993; Stuiver and Braziunas, 1993) was applied to all CFAMS ages. All ^{14}C ages are reported in calibrated years before present (cal BP) or calibrated years AD/BC (AD or BC) with a one-sigma (1σ) range of uncertainty.

Geospatial Data Sources

Geospatial processing and analysis were carried out using Esri's ArcGIS version 10.1. Core locations and GPR tracklines were overlaid atop orthorectified aerial imagery obtained from MassGIS, USGS quad sheets (also from MassGIS), and georeferenced historical maps, including an 1846 Coast Survey map (Boston Survey Consultants, 2007; Maio *et al.*, 2012; MassGIS, 2013). The Coast Survey maps (with a positional accuracy of ±10 m) have been deemed the most reliable and reproducible sources for coastal landscape features along the Massachusetts shoreline during the 19th century (Boston Survey Consultants, 2007; Giese, Mague, and Rogers, 2009; Mague, 2012; Maio *et al.*, 2012). The HWL was delineated on both the 2008 orthophotograph and 1846 Coast Survey map to compare and quantify coastal changes visually along the Waquoit barrier. The 1846 boundary of Flat Pond and adjacent coastal features (historic inlets and flood tidal delta) were also delineated. The location and width of buried paleochannels identified within the GPR data were also delineated, allowing for a determination of their spatial extent and relationship to other relict and historic subsurface features.

RESULTS

The results from the GPR and sediment core field work and lab analysis provide the foundation for our environmental interpretation of the barrier system. The images (radargrams) are used to differentiate major radar facies (RFs), which were observed along the entire length of the barrier. Core lithology was logged and delineated into seven main lithofacies (LFs), each representing a coastal environment existing in both ancient and modern settings.

Geophysical Database

The variability of sediment types along the barrier results in distinct layers of peat, sand, and gravel, although at some locations this variation is subtle. These layers show up in the radar data as sharp GPR reflectors that have allowed us to delineate individual RFs. We have identified six RFs from shore-parallel GPR data, including cut-and-fill, horizontal, subparallel, wavy-parallel, chaotic, and attenuated (Figure 3).

Radar Facies 1 (RF1)—Cut-and-Fill

RF1 is defined by a cut-and-fill structure incised into the barrier lithosome and bounded on the surface with continuous parallel to subparallel reflectors. RF1 is commonly bounded at the bottom by a concave-up reflector and generally exhibits a symmetrical geometry. Internal structure often consists of medium- to high-amplitude offlapping oblique sigmoidal reflectors that may extend in eastward or westward directions and sometimes converge in the center of the cut-and-fill sequence. Within RF1, imaged depths of more than 3 m were often achieved along the western portion of the barrier fronting Waquoit Bay, whereas along the eastern portion, fronting Sage Lot and Flat Ponds, much shallower depths (<2 m) were achieved by increased attenuation of the signal. Upper portions
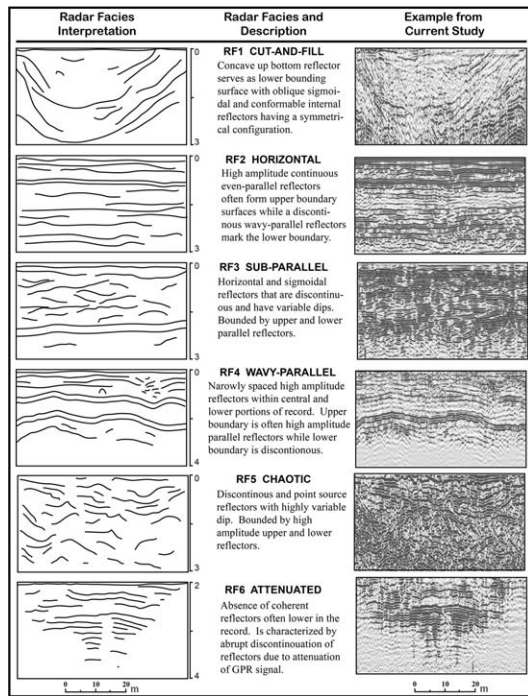
Figure 3. Six radar facies identified in GPR records along the Waquoit barrier beach. GPR profiles are shown on the right with interpretation on the left. The radar facies (RF) number, name, and summary are shown in the center column. Horizontal scales are shown at the bottom of radar profiles and interpretation. The depth scale relative to the ground surface varies and is shown left of interpretations in meters.

of RF1 in places contain smaller scale cut-and-fill sequences. The internal infill sequence with dipping clinoforms and chaotic discontinuous reflectors, combined with a nonconformity in the upper boundary, provides a signature for this facies, especially in areas where shallow attenuation prevents the imaging of tell-tail concave-up basal reflectors.

Radar Facies 2 (RF2)—Horizontal

The upper high-amplitude, even-parallel reflectors are continuous and often coincident with the ground surface. RF2 is present in all GPR data and is most commonly observed in the upper sediments. RF2 serves as the upper bounding surface to several other radar facies. High-amplitude horizontal reflectors are indicative of contrasts between sediment beds and are identified by an even and parallel continuous geometry. Sharp signal returns in the upper sediments can also signify the presence of the freshwater table.

Radar Facies 3 (RF3)—Subparallel

RF3 is subparallel and often bound by upper and lower parallel facies (RF2). Internal reflectors are horizontal to oblique and have variable dip angles and directions. The internal reflectors appear at high, moderate, and low amplitudes. Within the upper portions of RF3 are sometimes cut-and-fill structures that have a symmetrical geometry and small spatial scale when compared with RF1. Reflectors are continuous over short distances and lack symmetry in external form.

Radar Facies 4 (RF4)—Wavy-Parallel

High-amplitude wavy-parallel reflectors are observed in the center and lower portions of the record. In central portions of the record, RF4 is often continuous, whereas at deeper depths it is discontinuous because of attenuation of the GPR signal. RF4 is bound on the surface by parallel high-amplitude bounding surfaces (RF2). Lower bounding surfaces are often discontinuous because of attenuation of the GPR signal.

Radar Facies 5 (RF5)—Chaotic

RF5 is made up of medium-amplitude, discontinuous geometry having a nonsymmetrical internal configuration. The reflectors have variable dipping angles and directions. This facies sometimes contains small-scale hyperbolic signal returns and is bounded at the surface by continuous parallel to subparallel reflectors (RF2). The lower surface boundary has concave-up geometry.

Radar Facies 6 (RF6)—Attenuated

RF6 is marked by the attenuation of the radar signal. This facies makes up the lower boundary of all GPR profiles, especially in areas greater than 3 m depth. The reflector-poor RF6 can have a sharp contact with upper and adjacent bounding surfaces (RF2 and RF3). This facies if often characterized by a hard transition between a reflector-rich to a reflector-poor GPR facies, indicating an abrupt increase in signal attenuation (van Heteren et al., 1998).

Sediment Cores

The sediment cores obtained in this study (SCB1–SCB5), as well as WB1 and WB2 (Maio et al., 2014), ranged in depth below the surface between 4.2 and 5 m (Figure 4). Some uncertainties likely are associated with comparing the depths of the two sets of cores (SCB and WB), because the elevation of the beach surface may have changed considerably in the 2 years separating the two fieldwork campaigns. Sediment types identified within the cores included sand and gravels with some peat materials. Based on grain size, color, organic composition, and boundary distinctions, seven lithofacies were identified (LFA–LFG). LFA is the modern portion of the stratigraphy and is characteristic of the current backshore environment where the cores were taken. This facies varies in depth below the surface between 0.7 m (SCB5) and 1.5 m (SCB4) and consists of medium sand interbedded with coarse sediment and heavy-mineral horizons.

LFB has a sharp upper contact with LFA and is made up of peat. This well-defined facies can be correlated through all the cores. The peat thickness ranges between 15 cm (SCB5) and 30 cm (SCB3), and its depth from surface fluctuates between 75 cm (SCB1) and 125 cm (SCB4). Peat samples from LFB within WB2 were likely deposited within a brackish high salt marsh environment. Maio et al. (2014) concluded this on the basis of two indicators including the presence of *Distichlis spicata* rhizomes, which are associated with high salt marsh and disturbed environments, and the presence of foraminifera assemblages also indicative of a high marsh setting (Miller and Egler, 1950; Scott and Medioli, 1978). Foraminifera are ubiquitous in most marine environments and provide a good indicator of elevation and other environmental factors (Scott and Medioli, 1978; Murray, 2006). Species identified within the
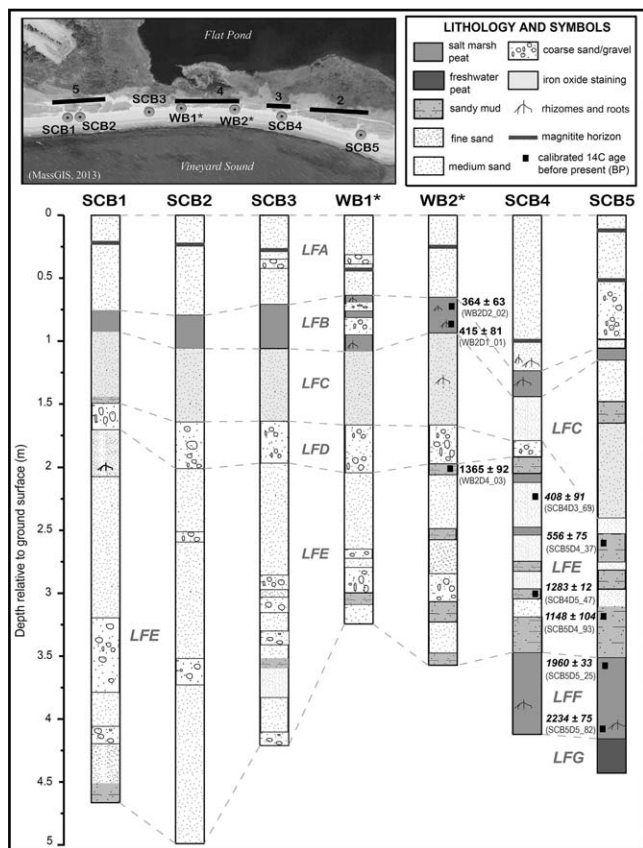
Figure 4. Core logs are shown with radiocarbon dates (solid black square) and lithofacies (LF) delineations (gray dashed line). All depths are relative to the ground surface. Seven distinct lithofacies were identified (LFA–LFG). WB1* and WB2* were collected by Maio et al., (2014) in 2011. SCB1 through SCB5 were collected in 2013. Location of individual cores (circles) in relation to buried inlet structures (solid black line) is shown in upper insert map (MassGIS, 2013). Lithology is shown in upper right legend. Radiocarbon ages are reported in calibrated years before present (cal BP) and shown with corresponding sample number (Table 2).

WB2 sample include *Haplophragmoides manilensis, Tiphotrocha comprimata,* and *Jadammina macrescens* (Maio *et al.*, 2014). Identification of rhizomes was carried out based on the descriptions and diagram contained within Niering, Warren, and Weymouth (1977). *D. spicata* has been shown to colonize areas of the coastal environments preferentially that have

become eroded by a high-energy event or upon peat layers that are in transition between fresh and salt hydrologic regimes (Miller and Egler, 1950). A sample of *D. spicata* from LFB at 78 cm yielded a date of 415 ± 81 cal BP (Maio *et al.*, 2014) (Table 1).

LFC consists of medium to fine sand having a reddish-yellow color (5RY 2/8) with woody roots. This lithofacies was observed in all cores, although within SCB4 the medium to fine sand does not have a reddish-yellow color. The color of the sand is characteristic of iron oxidation, indicating it was likely aerated. When coupled with the absence of foraminifera, the facies were likely subaerially exposed (Maio *et al.*, 2014). LFD consists of very coarse sand mixed with some gravel. LFD was not observed in the more eastern SCB5. The uppermost contact in LFD ranged in depth from surface between 1.5 m (SCB1) and 2.1 m (WB2) and in thickness between 20 cm (SCB1) and 35 cm (WB2). LFE is the dominant facies within the cores, consisting of beds of medium sand punctuated by very coarse sand and sandy mud horizons. Five radiocarbon ages were yielded from samples collected within LFE, with ages between 408 ± 91 and 1365 ± 92 cal BP (Table 1).

A deeper peat deposit in SCB4 and SCB5 is denoted as LFF. The facies spans between 3.4 and 4.3 m in depth. Two *D. spicata* rhizomes sampled from the upper (353–354 cm) and lower (410–411 cm) sections of this bed in SCB5 bracket LFF, with ages of 1960 ± 33 cal BP and 2234 ± 75 cal BP, respectively (Table 1). Within SCB5, the saltwater peat transitions to freshwater peat at 4.3 m; this is marked by a color change from black to brown and an absence of foraminifera and salt marsh rhizomes. The freshwater peat bed was designated LFG and had a sharp upper contact with LFF.

DISCUSSION

The integration of radar and core results, as well as information provided through previous research, allows for environmental interpretation of the radar facies and lithofacies contained within the Waquoit barrier system. These interpretations are ground truthed and supported with core stratigraphy. Three of the 13 buried paleochannels (3, 5, 12) identified are interpreted in detail and discussed. The combined information is used to assess the environmental evolution of Dead Neck and South Cape Beach along multiple spatial and temporal scales, providing context to ongoing and future changes enhancing society's ability to manage barrier systems effectively.

Table 1. *Radiocarbon results from nine samples selected from SCB and WB sediment cores. Asterisks indicate results from Maio* et al. *(2014). Bold data indicate median calibrated years before present with uncertainty value.*

Lab No.	Sample No.	C^{14} Method	Core	Depth (cm)	C^{14} Age	1-Sigma Probability	Median Cal BP (yr)	Material Dated
OS-106541	SCB5D4_93	CFAMS	SCB5	314–315	1490 ± 90	1044–1251	**1148 ± 104**	Shell matter
OS-106542	SCB5D4_37	CFAMS	SCB5	258–259	850 ± 90	481–630	**556 ± 75**	*Mya arenaria*, articulated
OS-106543	SCB4D3_69	CFAMS	SCB4	219–220	695 ± 95	317–498	**408 ± 91**	*M. arenaria*, articulated
OS-104585	SCB4D5_47	AMS	SCB4	289–290	1340 ± 25	1271–1295	**1283 ± 12**	Rootlet
OS-104587	SCB5D5_82	AMS	SCB5	410–411	2220 ± 25	2159–2309	**2234 ± 75**	*D. spicata* rhizome
OS-104588	SCB5D5_25	AMS	SCB5	353–354	2010 ± 30	1927–1993	**1960 ± 33**	Woody root
OS-94184*	WB2D2_02	AMS	WB2-D1	71–72	290 ± 25	301–426	**364 ± 63**	Bulk sediment
OS-94182*	WB2D1_01	AMS	WB2-D2	77–79	375 ± 25	334–496	**415 ± 81**	*D. spicata* rhizome
OS-94513*	WB2D4_03	AMS	WB2-D4	199–201	1480 ± 25	1340–1389	**1365 ± 92**	Woody root

Environmental Interpretations of Radar

The six radar facies (RF1–RF6) have characteristic geometry and signal strength, which allows for their categorization. Although a more detailed interpretation of radar facies could be carried out, the six facies interpreted here are generally representative of the subsurface architecture and stratigraphy along the Waquoit barrier and suffice to identify buried paleochannels and determine the geologic context in which they exist.

Radar Facies 1 (RF1)—Cut-and-Fill

RF1 represents the locations of buried cut-and-fill structures initially established through storm-driven breaching. RF1 includes both ephemeral breachways and more permanent tidal channels. In this study, a breachway is distinguished from a more permanent inlet by its shallower depth and shorter width (Mallinson *et al.,* 2010). Additionally, it is inferred that an active tidal inlet would result in the formation of a lag deposit and a concave-up lower bounding surface with a distinct channel-fill pattern (FitzGerald, Buynevich, and Rosen, 2001). The deeper penetration of the EM signal at locations containing RF1 suggests a greater permeability at these locations associated with larger sediment sizes, allowing for the seaward flow of fresh water. The presence of a shallow freshwater aquifer and increased penetrations is another indicator of RF1.

Seven primary types of channel-fill patterns were identified, with the majority of paleochannels exhibiting prograded, accretionary, and complex fill types (FitzGerald, Buynevich, and Rosen, 2001). Significant grain size transitions resulting from the internal structure of RF1 often present as well-defined oblique sigmoidal reflectors. Within these clinoform sets, each overlapping reflector represents a distinct phase of barrier aggradation or lateral migration (Buynevich and FitzGerald, 2001; van Heteren *et al.*, 1998). In areas where there are multiple paleochannel structures, as is the case along the eastern barrier, cut-and-fill sequences and clinoform sets can cross-cut external reflectors, indicating multiple inlet reincisions associated with repeated storm events.

Radar Facies 2 (RF2)—Parallel

RF2 was interpreted as representing modern beach deposits observed in the upper portions of the record combined with the presence of the freshwater table. The lithology of this radar facies can be correlated with LFA. High-amplitude, closely spaced reflectors signify distinctly layered medium sand, coarse sand, and heavy-mineral (primarily magnetite) horizons. The heavy-mineral horizons are erosional high-energy indicators.

Radar Facies 3 (RF3)—Subparallel

We interpret RF3 as a flood tidal delta or overwash deposit. The high- to middle-amplitude reflectors indicate high lithologic contrasts that result from the transition between fine and coarse sediments. This facies was primarily observed deeper in the record on the eastern portion of the barrier and associated with the presence of adjacent inlet structures. Based on the location and depth of RF3, it may coincide with LFE, with the medium-amplitude GPR reflectors corresponding to lithologic transitions between sandy mud; medium sand; and coarse-grain sand, gravel, or both.

Radar Facies 4 (RF4)—Wavy-Parallel

A high-amplitude wavy-parallel reflector indicates a signal-attenuating horizon such as peat or clay that has been deposited uniformly over an uneven paleotopography (van Heteren *et al.*, 1998). We interpret RF4 as a thin peat horizon denoted as LFB and LFF within the cores. Because peat typically attenuates the GPR signal, it can be assumed in cases where lower reflectors appear below RF4, that RF4 is a thin peat bed, thus allowing the radar to penetrate farther. The deeper, high-amplitude signal is indicative of a sharp transition between peat and sand beds. The presence of peat indicates that during its formation the barrier was likely seaward of its current position.

Radar Facies 5 (RF5)—Chaotic

RF5 is characteristic of a massive heterogeneous pile of sediments, possibly corresponding to unsorted outwash and glacial contact deposits. The minor hyperbolas in this facies stem from point reflectors such as larger clasts or boulders. These deposits are observed in paraglacial barrier settings, especially in areas of kettle formation (van Heteren *et al.*, 1998). RF5 is also indicative of anthropogenic modifications to the sediments. Sand and gravel fill commonly placed under roads or within breachways have a chaotic reflector pattern. Because the Waquoit barrier was used as a training ground for amphibious landings during WWII (Keay, 2001), it is likely that some portions of the barrier have been significantly modified and filled, which could explain the presence of RF5 at some locations.

Radar Facies 6 (RF6)—Attenuated

We interpret RF6 as areas of the record where the GPR signal is attenuated because of the presence of saltwater or salt marsh peat or clay. Saltwater attenuates the GPR signal in coastal settings, but the presence of a freshwater lens above the salt water along barrier beaches permits signal penetration. RF6 can provide information about the depth of the saltwater table and presence of freshwater aquifers (van Heteren *et al.*, 1998). Along the Waquoit barrier, several sets of parallel reflectors abruptly discontinue both laterally and vertically. This likely indicates the seaward flow of freshwater into a surrounding zone of brackish and salty groundwater. Additionally, a sharp discontinuation of high-amplitude lower reflectors can signify the presence of large peat deposits. In this way, RF6 can serve as a tool to map the spatial extent of subsurface attenuating features and, in the presence of freshwater aquifers, can serve to help identify buried channel structures.

Lithology

The LFA sediments are characteristic of the present backshore environment where the cores were collected. The medium sand making up the majority of sediments in this facies is interbedded with storm-deposited coarse-grain sands and heavy-mineral (primarily magnetite) horizons. Stemming from the depth in core of these deposits and the age model, it is likely these coarse-grain horizons are associated with recent storm events. The peat horizon denoted LFB is continuous
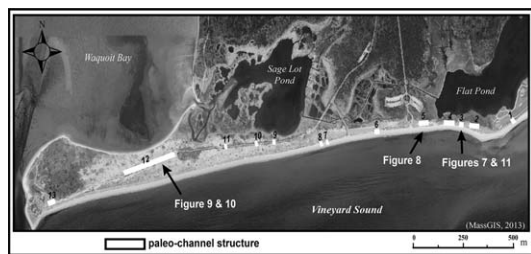
Figure 5. Thirteen buried relict inlets identified with ground-penetrating radar. The approximate positions of Paleochannels 1 through 13 are delineated with dark bold lines. Figure numbers corresponding to buried relict inlets are shown in white.

through all of the cores. The presence of peat at this depth was useful in identifying the paleoenvironmental evolution of the site, in that it contained *D. spicata* rhizomes and foraminifera assemblages indicative of a high salt marsh environment.

Based on the mix of fine to medium sand, rootlets, and reddish-yellow color, LFC is interpreted as dune sand. Sediments with similar physical characteristics can be observed today along the low-lying dune system of Dead Neck. LFD is inferred to be a lag sequence that makes up the lower bounding surface of cut-and-fill sequences (RF1). Gravel lag sediments form as a result of concentrated tidal flow at the throat of tidal channels and are a diagnostic feature for buried relict inlets in glaciated settings (FitzGerald, Buynevich, and Rosen, 2001). These deposits can form both within and adjacent to the throat of active tidal inlets.

LFE is characteristic of a back-barrier depositional area formed adjacent to tidal channels such as flood tidal deltas or overwash fans. The medium sand making up the dominant sediment type within LFE likely arrived from seaward sources such as the adjacent shoreface and ebb-tidal deltas during periods of normal inlet activity. Within these settings, sandy mud is subaqueously deposited during more quiescent periods, whereas coarse sediments are deposited during higher energy storm events (Mallinson *et al.*, 2010). This results in a lithostratigraphy composed of interbedded medium sand with smaller horizons of sandy mud and very coarse sand. These horizons do not correlate at depth when compared through all the cores, indicating that these sequences are highly localized and dependent on adjacent conditions, such as the presence or absence of an active inlet.

LFF is interpreted as a salt marsh that, based on radiocarbon ages, existed between 1960 and 2234 cal BP. The absence of LFF in the five more western cores indicates lateral variability in the back-barrier environments that once existed at South Cape Beach. The sharp contact between LFF and LFG indicates a rapid transition between fresh and saline environments at this location. The radiocarbon age returned from the bottom of Unit F of 2234 ± 75 cal BP indicates that the transition to a brackish system had occurred by this point in time. This fresh to brackish transition is coincident with the one recorded within the sediments of nearby Hamblin Pond, where the first salt marsh signature overriding a freshwater
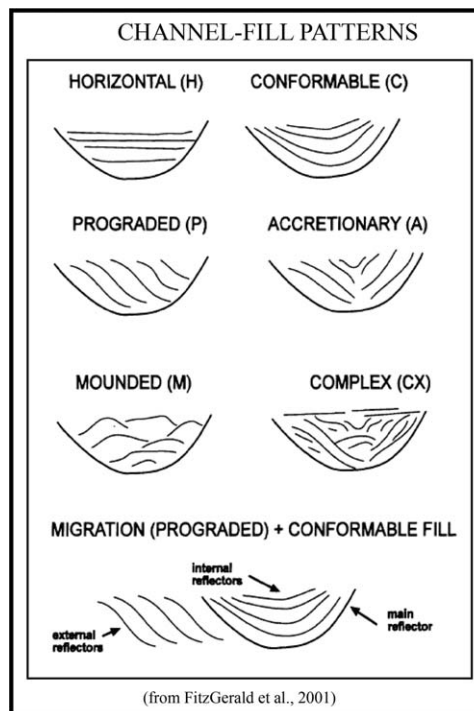

Figure 6. Channel-fill patterns outlined by FitzGerald, Buynevich, and Rosen (2001) and applied in this study.

swamp appears at approximately 2300 BP (Orson and Howes, 1992).

Identification of Buried Paleochannel Structures

The interpretation of paleochannel sequences was based on the configuration, geometry, and amplitude of reflectors using the 500-MHz antenna (FitzGerald, Buynevich, and Rosen, 2001; van Heteren *et al.*, 1998). The sediment cores taken along South Cape Beach allowed for the ground truthing of radar data in this area. Facies transitions correlated with abrupt contacts between lithofacies when significant lithologic contrasts were present. Because of a lack of cores along the remainder of the barrier, the stratigraphy in these areas is based primarily on interpretation of radar data (FitzGerald, Buynevich, and Rosen, 2001; van Heteren *et al.*, 1998).

Thirteen paleochannel sequences were identified and denoted as Paleochannels 1 through 13 (Figure 5). Six channel fill patterns characterized by FitzGerald, Buynevich, and Rosen (2001) were observed (Figure 6). Paleochannels ranged in width between 16 and 275 m, with depths between 1.3 and 3.7 m (Table 2). The combined width of the buried channel structures totaled 704 m, making up 24% of the 2.9-km barrier lithosome.

Paleochannels 1–5 are located along the eastern portion of South Cape Beach. The beach is made up of a narrow barrier fronting Flat Pond in close vicinity to historically active inlets delineated on the 1846 Coast Survey map, as well as the paleoforest documented by Maio *et al.* (2014). Increased attenuation of the EM signal along this portion of the barrier,

Table 2. *Thirteen paleochannels delineated from radar data. Inlet number, GPR line number, center location, and geometry shown. Channel-fill pattern derived from FitzGerald, Buynevich, and Rosen (2001).*

Paleochannel No.	Survey Line No.	Longitude (W)	Latitude (N)	Width (m)	Depth below Surface (m)	Channel-Fill Pattern
1	5-2012	70°29.522	41°33.167	24	2.2	Complex
2	6-2012	70°29.718	41°33.134	60	2.5	Accretionary/complex
3	6-2012	70°29.792	41°33.144	27	2.3	Accretionary
4	8-2012	70°29.826	41°33.146	64	1.9	Conformable
5	8-2012	70°29.94	41°33.145	60	2.8	Accretionary
6	3-2012	70°30.143	41°33.121	30	2.3	Mounded
7	11-2010	70°30.356	41°33.093	16	1.3	Prograding
8	11-2010	70°30.382	41°33.088	20	1.3	Accretionary/horizontal
9	12-2010	70°30.587	41°33.09	20	2.54	Complex
10	818-2013	70°30.684	41°33.084	77	2	Horizontal
11	12-2010	70°30.795	41°33.076	17	2.8	Horizontal
12	815-2013	70°31.139	41°33.018	275	3.7	Prograding/complex
13	814-2013	70°31.550	41°32.928	47	2.4	Prograding

as well as the presence of multiple closely spaced cut-and-fill sequences, made deciphering individual paleochannel facies difficult despite the core data.

The small spatial extent of many of the cut-and-fill sequences identified in this study (3 and 7–11) suggests they were likely short-lived ephemeral breachways that closed shortly after their formation. Five of these more ephemeral paleochannels were located along the wider portions of the barrier, such as those areas fronting Sage Lot Pond. In these areas, sand dunes and salt marsh result in the barrier being significantly wider than the eastern and western segments. When a large storm event breaches the barrier at these locations, the resulting breachway is likely unable to capture the back-barrier tidal prism. This leads to conditions in which the rate of longshore sediment transport and lateral infilling exceeds transport in and out of the inlet, leading to eventual closure (FitzGerald, Buynevich, and Rosen, 2001). The more established paleochannel facies (1, 2, 4–6, 12, and 13) exhibit a greater spatial extent, exhibit a concave up bottom reflector, and primarily only occurred on the far eastern and western portions of the barrier.

Paleochannel 3

Paleochannel 3 was approximately 14 m in width and 1.4 m in depth (Figure 7). A high-amplitude reflector is observed at a depth of 1.2 m. We attribute this reflector to the high marsh peat horizon making up SCB4 LFB (114–134 cm). Above this, radar reflectors exhibit a sigmoidal-oblique configuration characteristic of an accretionary pattern of channel fill. The accretionary channel fill occurs in the upper meter of sediments and can be linked through cores to LFA.

We interpret Paleochannel 3 as a short-lived breachway that failed to capture a significant portion of the back-barrier tidal prism because of its small spatial extent. The shallow depth of Paleochannel 3, as well as the presence of the slumping peat horizon (LFB and RF4), indicates that the upper sequence was possibly incised into deeper and older paleochannels. Based on the age of the *D. spicata* rhizomes from WB2, the upper inlet sequence occurred some time after 415 ± 81 cal BP (Table 2). Based on this temporal constraint, and its location, Paleochannel 3 is inferred to be the remnant of the middle inlet depicted on the Coast Survey map (Figure 2). Because the inlets are delineated above the HWL on the Coast Survey map, it is inferred that they no longer were active during this time

and had already begun to fill. This places their time of formation sometime before 1846.

Paleochannel 5

Paleochannel 5 was one of the larger cut-and-fill structures identified in this study with a width of 60 m and depth of 2.5 m (Figure 8). A high-amplitude, concave-up bottom reflector marks the lower bounding surface for this paleochannel structure. Based on SCB1 and SCB2 core lithology, this reflector coincides with the coarse sand and gravel composing LFD. A lower amplitude, concave-up reflector falls directly above the lower bounding surface and is recorded between 0.8 and 1 m, aligning closely with LFB (peat) and RF4. Oblique sigmoidal reflectors are dipping in both eastern and western directions with an accretionary pattern of fill. Depth correlations between radar reflectors and core lithology indicate that a portion of the channel fill likely corresponds to dune sand denoted as LFC.

When taken together, the paleochannel's structure, large size, and accretionary fill pattern indicates it was likely a relatively long-lived feature at this location. Longer lived inlets such as this will often remain active until a new inlet is opened nearby that captures the back-barrier tidal prism, causing the infilling of the former inlet. Unlike the more eastern paleochannels (1–4) that likely existed during the historic period, Paleochannel 5 had a much larger spatial extent and well-defined geometry. Because no channels are delineated at this location on historic or modern maps, Paleochannel 5 is inferred to have existed during the early historic to prehistoric period.

Paleochannel 12

Paleochannel 12 was the largest cut-and-fill sequence identified in this study. The total width of the sequence is approximately 275 m, with a depth below the surface of 3.7 m (Figure 9). A prominent high-amplitude reflector that is concave-up in the center of the sequence is observed at 3.7 m, marking the base of the inlet. A series of oblique sigmoidal clinoforms dip from both eastward and westward directions, indicating progradation and lateral infilling.

Within the central portion of the paleochannel sequence chaotic reflectors dominate, indicating the presence of RF5. Closer to the surface (0.8 m), a high-amplitude reflector is continuously present across the length of the paleochannel sequence and has a distinct concave-up feature directly
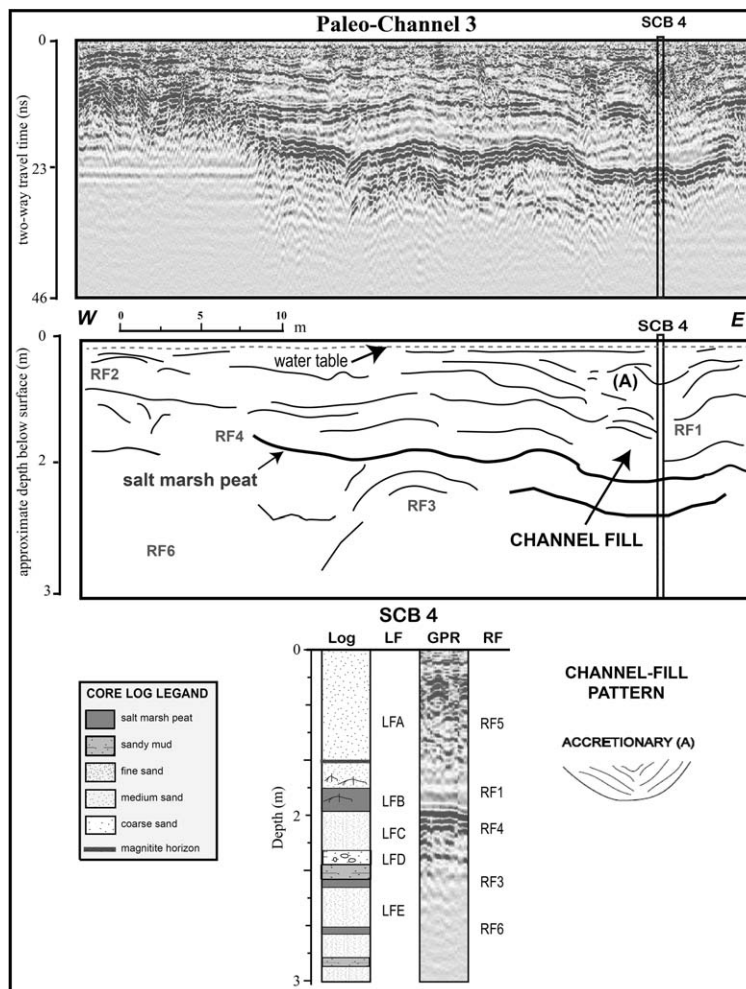
Figure 7. Radar profile of Paleochannel 3 shown with SCB4 sediment core location and interpretation. The upper 2 m of the SCB4 core log and corresponding radar reflectors are also shown with depth scale on left. Within interpretation box radar facies (RFs) are identified. Corresponding lithofacies (LFs) and RFs are shown next to core log and radar section. Lithologic symbols are shown in legend and LF is shown next to the core corresponding to core stratigraphy. The high-amplitude reflector at 1.2 m is linked to the high marsh peat horizon identified as LFB. Configuration of radar reflectors is characteristic of an accretionary channel fill pattern.

overlying the channel fill on the eastern and western ends of the sequence. Based on the depth and amplitude of this reflector (RF3), it is inferred that it represents a peat horizon similar to what was observed at the same depth within Paleochannel 5 and verified with cores as LFB.

Because of supporting evidence, Paleochannel 12 is interpreted as once being a major inlet connecting Waquoit Bay to the Vineyard Sound that shifted position in both eastward and westward directions through time (Figure 10). Based on its size (275 m) and depth (3.7 m), the paleochannel that once existed at this location likely captured a significant portion of Waquoit Bay's tidal prism, which would explain its large size and depth. During its existence, it likely was more comparable in width to the historic main channel delineated on the Coast Survey map. From its location, we infer that the main entrance connecting Waquoit Bay to the Vineyard sound was located a minimum of 650 m east of its current position sometime before 1846. The

hydrographic constraints on inlet size make it unlikely that the present main channel and Paleochannel 12 were both active at the same time. It is likely that the infilling and closure of Paleochannel 12 allowed conditions to exist for the formation of a new inlet in the vicinity of the present waterway.

In addition to the internal geometry of Paleochannel 12, there are also surficial features in the modern environment, indicating a major channel once existed at this location. Paleochannel 12 coincides with a major back-barrier channel feature that impinges on the rear portion of the present barrier, indicating that a high-energy erosional environment existed at this location in the past (Figure 10C). FitzGerald, Buynevich, and Rosen (2001) identified a similar feature directly landward of a 200-m-wide subsurface paleochannel structure located along Duxbury Beach. This buried inlet was likely a long-lived channel that had fully captured a significant portion of the embayment's tidal prism, resulting in the scouring of the
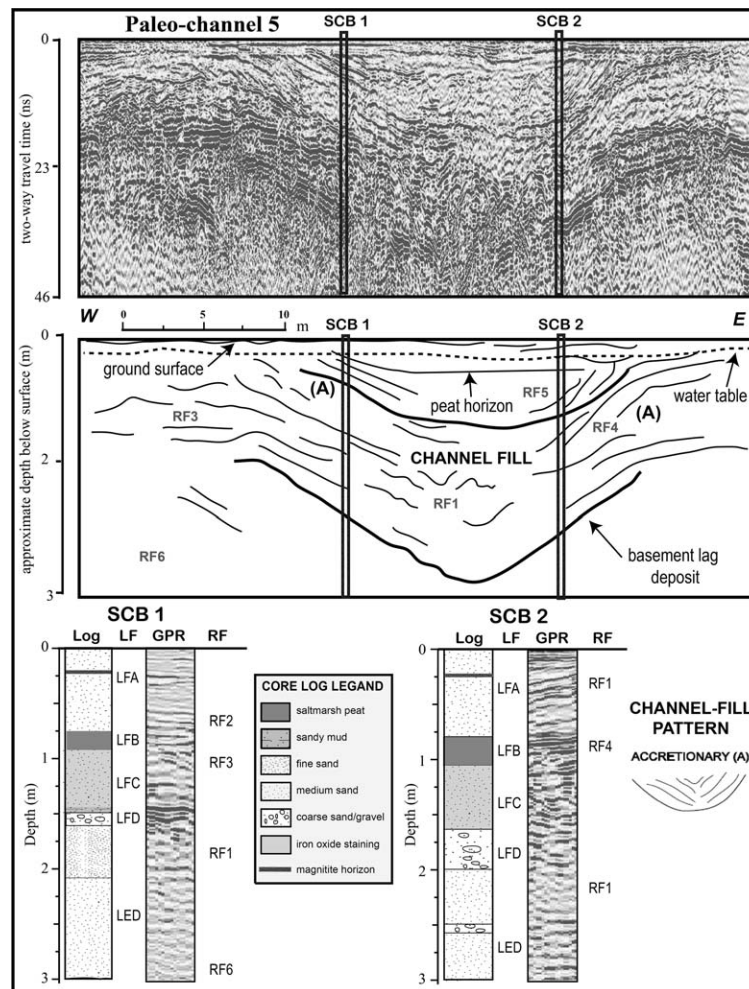
Figure 8. Radar data and interpretation of Inlet 5 shown with the location of SCB1 and SCB2 cores. All depths are relative to ground surface. Interpreted radar facies (RFs) are identified. An accretionary (A) channel-fill pattern is observed on the east and west sides of the paleochannel with key on lower left from FitzGerald, Buynevich, and Rosen (2001). Core logs and corresponding radar sections are shown with lithofacies (LF) designation. Radar sections approximately corresponding to core location are shown to right of core logs with RF interpretation. Lithology legend is shown in center.

adjacent bay tidal channel (FitzGerald, Buynevich, and Rosen, 2001). Additionally, the HWL delineated from the Coast Survey map indicates that more than 20 m of seaward accretion has occurred adjacent to the subsurface inlet feature since 1846 (Figure 10B). The former position of the HWL indicates the barrier was at one time considerably narrower at this location, making it more likely to have contained a channel.

Rapid Coastal Change along South Cape Beach Characteristic of Regional Trends

Abundant data demonstrate that dramatic coastal changes have occurred along the portion of the South Cape Beach fronting Flat Pond (*Maio et al.*, 2014) (Figure 11). New data presented in this study indicate that the area is riddled with former inlets and breachways, with a minimum of five paleochannel facies (1–5) delineated from radar data at this location. The presence of subfossil stumps within the shallow shoreface indicates a landward shift in coastal environments at

this location for at least the past 1200 years (Maio *et al.*, 2014). Cores taken along the fringing marsh of Flat Pond directly landward of the paleoforest site contain a 500-year record of breaching and overwash events (Maio *et al.*, 2014) and offer supportive evidence of rapid fluctuations between saline and freshwater regimes within Flat Pond (Orson and Howes, 1992).

The correlation between buried inlet structures and shoreline change has major implications for coastal zone management, as there is a growing body of evidence that links underlying geology with shoreline morphology and evolution (Belknap and Kraft, 1985; McNinch, 2004). Along the barrier islands of North Carolina, Browder and McNinch (2006) determined that a direct linkage exists between relict inlets buried beneath the modern shoreface and hotspot areas of anomalous coastal change. Evidence also suggests that the rate of transgression is accelerating along this section of the beach. Between 1846 and 2008, the shoreline retreated landward by 70 m at a long-term rate of 0.43 m/y (Maio *et al.*, 2014).
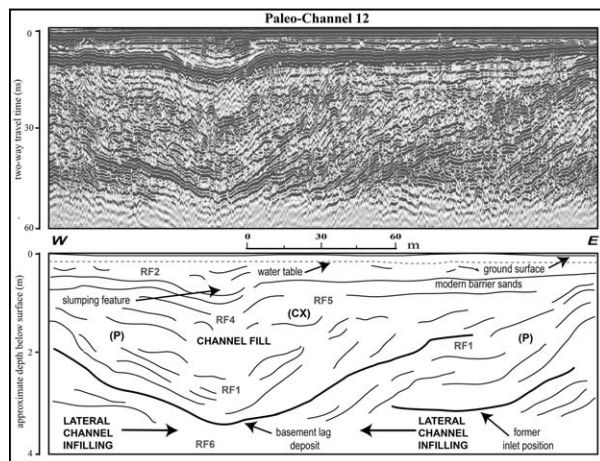
Figure 9. GPR profile and interpretation for Inlet 12. Radar facies (RF) and fill type is delineated on the interpretation. This was the largest inlet structure identified in this study, reaching an approximate width of 275 m and depth of 3.7 m relative to the ground surface. The profile has been vertically exaggerated. A high-amplitude concave-up reflector shown with the bold black line marks the prefilled basement of the inlet. Oblique sigmoidal reflectors trend in both eastward and westward directions. The inlet had a progradational (P) fill on its eastern and western sides and a complex (CX) fill pattern within its center. The inlet likely represents a major paleochannel connecting Waquoit Bay to the Vineyard Sound.

Furthermore, first-hand observations during both Hurricane Sandy and the February Blizzard of 2014 documented a loss of 3–5 m of the narrow dune belt fronting Flat pond and the golf course.

The destabilization of barrier systems in response to accelerated rates of sea level rise coupled with high-energy storm events has been observed along coastal barriers along the U.S. East Coast and the Gulf of Mexico (Ashton, Donnelly, and Evans, 2008; Mallinson *et al.,* 2011; Seminack and Buynevich, 2001). Numerous studies have shown that coastal barriers are rapidly migrating landward and degrading (FitzGerald, Buynevich, and Rosen*,* 2001; FitzGerald *et al.,* 2007; Khalil, Finkl, and Raynie, 2013; Mallinson *et al.,* 2010; Williams, Penland, and Sallenger*,* 1992). Mallinson et al. (2010) collected more than 200 km of GPR data along the Outer Banks barrier island system of North Carolina and identified multiple transgressive facies in the subsurface sediments. The formation of multiple cut-and-fill sequences identified in GPR images is linked to heightened storm activity recorded during the Little Ice Age and Medieval Warm Period (Mallinson *et al.,* 2011). This research highlights the vulnerability of coastal barriers to storm-driven breaching events during past, and conceivably future, perturbations in global climate change.

Age Control for Inlet Formation

The third objective of this study was to develop age control for the formation and closing of relict inlets. This proved difficult due to a number of factors, including the absence of core data along Dead Neck, limited organic material for radiocarbon dating within the lower bounding surfaces of paleochannel sequences, and an absence of accurate historic maps before
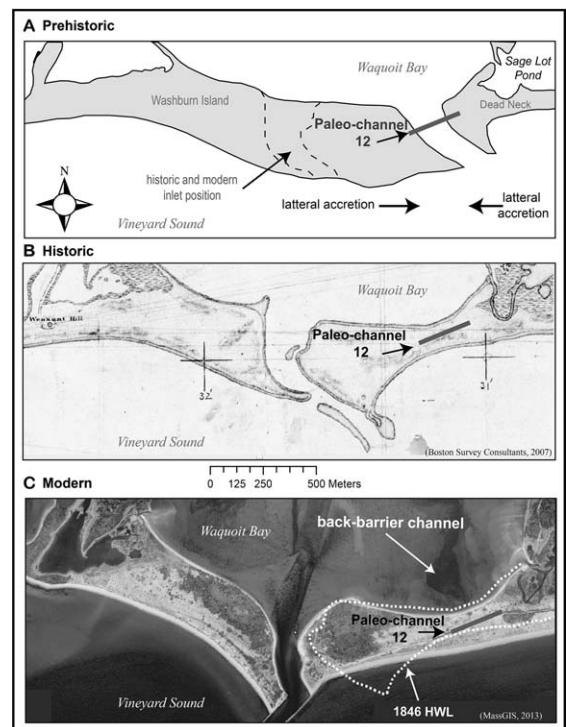

Figure 10. Morphologic evolution of the Waquoit barrier in the vicinity of Dead Neck and Washburn Island. (A) Conceptual model of prehistoric configuration with interpreted main channel location based on position of Paleochannel 12 shown with dark gray line. The general location of both the modern and historic inlet is shown with the white dashed line. Horizontal arrows indicate the lateral migration and infilling of the former inlet. (B) 1846 Coast Survey map with position of Paleochannel 12 shown with black line (Boston Survey Consultants, 2007). (C) A 2011 orthophotograph with current barrier configuration. The 1846 high water line (HWL) is shown with the white dashed line. The position of Paleochannel 12 is identified with a black line adjacent to a back-barrier channel feature interpreted to be a surficial indicator of the prehistoric inlet.

1846. A limited budget prevented the use of optical stimulated luminescence dating, which would have greatly improved age control for the formation of inlet features (Mallinson *et al.,* 2010). Despite the limited age control, some inferences can be made that can aid in the temporal understanding of the evolution of the Waquoit barrier.

Based on the Coast Survey map, the formation of the buried inlets documented in this study occurred sometime before 1846. The well-defined morphology of the main channel connecting Waquoit Bay to the Vineyard Sound, as delineated on the Coast Survey map (Figure 2), indicates that its position was well established by this point in time. The presence of the back-barrier channel adjacent to Paleochannel 12 (Figure 10C) also provides some constraint on the timing of its closure because coastal processes would likely result in its eventual infilling if a considerable amount of time had passed. This places the timing of closure of Paleochannel 12 and the opening of the current channel some time in the early historic (post-1620) to prehistoric period.
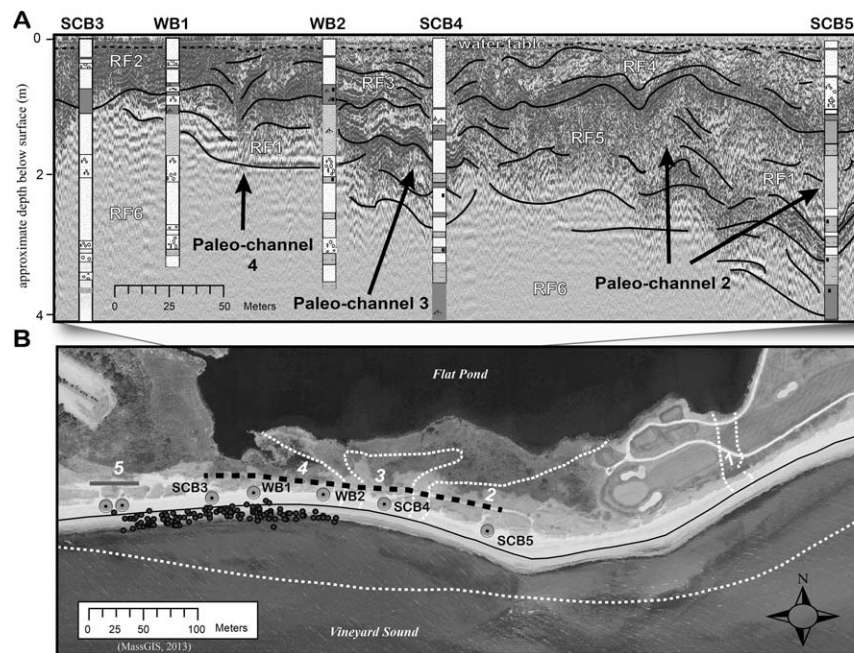
Figure 11. Evidence of dramatic coastal change along South Cape Beach. (A) Radar data for segment of beach shown with the black dashed line in lower map. The profile has been exaggerated 30× on the vertical scale. Radar data are interpreted with the white lines, with inlets 2, 3, and 4 identified. Radar facies (RF) interpretation is identified with white letters, including RF1—Cut-and-Fill, RF2—Horizontal, RF3—Subparallel, RF4—Wavy-Parallel, RF5—Chaotic, and RF6—Attenuated. SCB and WB sediment cores are exaggerated horizontally and shown overlaid on interpreted radar data. Core lithology symbols are shown in Figure 3. (B) A 2008 orthophotograph (MassGIS, 2013) of site showing inlet number, sediment cores (circles), 2008 HWL (black line), 1846 HWL (white dashed line), and paleoforest subfossils (small black circles). The narrowness of this portion of the barrier and its history of environmental change make it highly susceptible to future storm-driven breaching.

Based on their delineated position above the HWL on the Coast Survey map, the historic inlets fronting Flat Pond (Paleochannels 1–4) were becoming less active by 1846, indicating their formation likely occurred years to decades earlier (Figure 11). The presence of these inlets would likely have prevented hydrographic conditions to exist that would allow for an additional active channel, such as Paleochannel 5 (Figure 8). Because of Paleochannel 5's large size, depth, and absence of surficial back-barrier indicators, it is inferred that it was formed sometime during the early historic to late prehistoric period. The paleoforest that sits directly seaward of Paleochannel 5 existed until 1530 ± 82 AD (Maio *et al.,* 2014); thus, the formation of the inlet likely came after this point in time.

Between 1620 and 1846 two major hurricanes severely impacted the Massachusetts coastline, leading to the wide-scale breaching and overwash events (Boldt *et al.,* 2010; Boose, Chamberlin, and Foster, 2001; Buynevich and Donnelly, 2006; Ludlum, 1963). These included the Great September Gale of 1815 and the Great Colonial Hurricane of 1635 (Ludlum, 1963). The Great September Gale was the largest of the 19th century, making landfall along the Connecticut coastline (Boldt *et al.,* 2010; Boose, Chamberlin, and Foster, 2001). To the west, the southern-facing bays of Rhode Island and Massachusetts took the brunt of the storm surge as peak wind speeds came coincident with high tide (Ludlum, 1963). The Great Colonial Hurricane of 1635 is the first hurricane documented in the

historical record and was said to have resulted in storm surges within Buzzards Bay exceeding 6 m (Boldt *et al.,* 2010; Ludlum, 1963). The devastation resulting from the 1635 hurricane was not seen again until the September Gale of 1815, 180 years later (Ludlum, 1963). These hurricanes would be the most likely mechanisms for the formation of some of the paleochannels identified in this study, with the 1815 event potentially resulting in the opening of new inlets along South Cape Beach, and the earlier 1635 event leading to the formation of Paleochannel 5 and closure of Paleochannel 12. It is also possible that prehistoric storm events that have been archived in nearby salt marsh sediments (Boldt *et al.,* 2010; Donnelly *et al.,* 2001; Scileppi and Donnelly, 2007) could also have played a role.

CONCLUSIONS

In this study, we have utilized GPR and sediment cores to determine the location, internal geometry, and channel-fill patterns of buried inlet structures. GPR has proved to be a viable imaging tool along the Waquoit barrier system, where mixed sediment composition and the presence of a freshwater lens produced clear bounding surfaces between lithological units. This has increased our knowledge concerning the distribution of coastal segments vulnerable to breaching events and illuminated the morphologic evolution of the barrier. The results provide a complementary database that can be

integrated into a regional framework of late Holocene storm-driven change.

The Waquoit barrier has a minimum of 13 cut-and-fill structures making up 24% of the barrier lithosome. Radar reflector configurations are characteristic of both ephemeral breachways and more permanent tidal channels. Six distinct radar facies were identified, and sediment cores served to define seven lithofacies and to ground truth the radar data. A total of seven channel-fill patterns were assigned to paleo-channel structures based on reflector configuration, with accretionary, prograding, and complex patterns being the most common. The extent of historic and prehistoric inlets along the Waquoit barrier demonstrate that these features are an important component of transgressing barrier systems (Fitz-Gerald, Buynevich, and Rosen, 2001; Seminack and Buynevich, 2013).

The late Holocene formation of paraglacial coastal barriers occurred as a result of a deceleration of sea level rise, making them highly vulnerable to accelerated rates of sea level rise and increased storminess in the future. Continued sea level rise will seriously affect the stability of barrier systems globally and will likely result in an increase in breaching events and changes to inlet configurations (Ashton, Donnelly, and Evans, 2008). This study has shown that morphologic and environmental changes are already being observed along South Cape Beach, which mirrors regional trends of barrier retreat and deterioration (FitzGerald, Buynevich, and Rosen, 2001; FitzGerald *et al.,* 2007; Khalil, Finkl, and Raynie, 2013; Mallinson *et al.,* 2010; Williams, Penland, and Sallenger, 1992). In the coming decade, coastal barrier systems will likely experience rapid morphologic and environmental change, including the salinization of freshwater systems and increased storm-driven overwash, breaching, and flooding events (Ashton, Donnelly, and Evans, 2008; FitzGerald *et al.,* 2007). These factors will undoubtedly have negative consequence to both natural and human systems and, thus, demand further research that guides the implementation of appropriate mitigation and adaptation strategies.

LITERATURE CITED

Ashton, A.D.; Donnelly, J.P., and Evans, R.L., 2008. A discussion of the potential impacts of climate change on the shorelines of the northeastern USA. *Mitigation and Adaptation Strategies for Global Change*, 13(7), 719–743.

Balco, G.; Stone, J.O.; Porter, S.C., and Caffee, M.W., 2002. Cosmogenic-nuclide ages for New England coastal moraines, Martha's Vineyard and Cape Cod, Massachusetts, USA. *Quaternary Science Reviews,* 21(20), 2127–2135.

Barbier, E.B., 2012. Progress and challenges in valuing coastal and marine ecosystem services. *Review of Environmental Economics and Policy*, 6(1), 1–19.

Barbier, E.B.; Hacker, S.D.; Kennedy, C.; Koch, E.W.; Stier, A.C., and Silliman, B.R., 2011. The value of estuarine and coastal ecosystem services. *Ecological Monographs*, 81(2), 169–193.

Belknap, D.F.; Gontz, A.M., and Kelley, J.T., 2005. Paleodeltas and preservation potential on a paraglacial coast—evolution of eastern Penobscot Bay, Maine. *In:* FitzGerald, D.M. and Knight, J., (eds.), *High Resolution Morphodynamics and Sedimentary Evolution of Estuaries*. Dodrecht, The Netherlands: Springer, pp. 335–360.

Belknap, D.F. and Kraft, J.C., 1985. Influence of antecedent geology on stratigraphic preservation potential and evolution of Delaware's barrier systems. *Marine Geology*, 63(1), 235–262.

Boldt, K.V.; Lane, P.; Woodruff, J.D., and Donnelly, J.P., 2010. Calibrating a sedimentary record of overwash from southeastern New England using modeled historic hurricane surges. *Marine Geology,* 275(1–4), 127–139.

Boose, E.R.; Chamberlin, K.E., and Foster, D.R., 2001. Landscape and regional impacts of hurricanes in New England. *Ecological Monographs,* 71(1), 27–48.

Boston Survey Consultants, 2007. *Massachusetts Chapter 91 Mapping Project. Final Report*. Norwell, Massachusetts: BSC Group, 78p.

Browder, A.G. and McNinch, J.E., 2006. Linking framework geology and nearshore morphology: Correlation of paleo-channels with shore-oblique sandbars and gravel outcrops. *Marine Geology*, 231(1), 141–162.

Buynevich, I., 2003. Subsurface evidence of a pre-1846 beach across Menauhant barrier, Cape Cod, Massachusetts. *Shore and Beach*, 71(3), 3–6.

Buynevich, I.V. and Donnelly, J.P., 2006. Geological signatures of barrier breaching and overwash, southern Massachusetts, U.S.A. *In:* Buynevich, I.V. and Donnelly, J.P. (eds.), *Proceedings of the 8th International Coastal Symposium (ICS 2004)*, Vol. I (Winter 2006), Journal of Coastal Research, Special Issue No. 39, pp. 112–116.

Buynevich, I.V. and FitzGerald, D.M., 2001. Styles of coastal progradation revealed in subsurface records of paraglacial barriers: Duxbury, Massachusetts, USA. *In:* Buynevich, I.V. and FitzGerald, D.M. (eds.), *International Coastal Symposium (ICS 2000): Challenges for the 21st Century in Coastal Sciences, Engineering and Environment*, Journal of Coastal Research, Special Issue No. 34, pp. 194–208.

Buynevich, I.V. and Fitzgerald, D.M., 2003. High-resolution subsurface (GPR) imaging and sedimentology of coastal ponds, Maine, USA: Implications for Holocene back-barrier evolution. *Journal of Sedimentary Research*, 73(4), 559–571.

Buynevich, I.V.; FitzGerald, D.M., and van Heteren, S., 2004. Sedimentary records of intense storms in Holocene barrier sequences, Maine, USA. *Marine Geology*, 210(1), 135–148.

Donnelly, J.P.; Bryant, S.S.; Butler, J.; Dowling, J.; Fan, L.; Hausmann, N.; Newby, P.; Shuman, B.; Stern, J.; Westover, K., and Webb, T., III, 2001. 700 yr sedimentary record of intense hurricane landfalls in southern New England. *Geological Society of America Bulletin*, 113(6), 714–727.

Donnelly, J.P.; Butler, J.; Roll, S.; Wengren, M., and Webb, T., III, 2004. A backbarrier overwash record of intense storms from Brigantine, New Jersey. *Marine Geology,* 210(1), 107–121.

FitzGerald, D.M.; Kulp, M.; Hughes, Z.; Georgiou, I.; Miner, M.; Penland, S., and Howes, N., 2007. Impacts of rising sea level to backbarrier wetlands, tidal inlets, and barrier islands: Barataria coast, Louisiana. *Proceedings of Coastal Sediments 07* (New Orleans, Lousisiana: ASCE), pp. 179–1192.

FitzGerald, D.M.; Buynevich, I.V., and Rosen, P.S., 2001. Geological evidence of former tidal inlets along a retrograding barrier: Duxbury Beach, Massachusetts, USA. *In:* Buynevich, I.V. and FitzGerald, D.M. (eds.), *International Coastal Symposium (ICS 2000): Challenges for the 21st Century in Coastal Sciences, Engineering and Environment*, Journal of Coastal Research, Special Issue No. 34, pp. 437–448.

FitzGerald, D.M.; Fenster, M.S.; Argow, B.A., and Buynevich, I.V., 2008. Coastal impacts due to sea-level rise. *Annual Review of Earth and Planetary Sciences*, 36(May 2008), 601–647.

Fitzgerald, D.M.; and van Hetteren, S., 1999. Classification of paraglacial barrier systems: Coastal New England, USA. *Sedimentology*, 46, 1083–1108.

FitzGerald, D.M.; van Heteren, S., and Montello, T.M., 1994. Shoreline processes and damage resulting from the Halloween Eve storm of 1991 along the north and south shores of Massachusetts Bay, USA. *Journal of Coastal Research*, 10(1), 113–132.

Giese, G.S.; Mague, S.T., and Rogers, S.S., 2009. *A Geomorphological Analysis of Nauset Beach/Pleasant Bay/Chatham Harbor for the Purpose of Estimating Future Configurations and Conditions.* Prepared for The Pleasant Bay Resource Management Alliance. Provincetown, MA: Provincetown Center for Coastal Studies, 32p.

Gontz, A.M.; Maio, C.V.; Wagenknecht, E.K., and Berkland, E.P., 2011. Assessing threatened coastal sites: Applications of ground-penetrating radar and geographic information systems. *Journal of Cultural Heritage*, 12(4), 451–458.

Gutierrez, B.; Uchupi, E.; Driscoll, N., and Aubrey, D., 2003. Relative sea-level rise and the development of valley-fill and shallow-water sequences in Nantucket Sound, Massachusetts. *Marine Geology*, 193(3), 295–314.

Hayes, M.O., 1980. General morphology and sediment patterns in tidal inlets. *Sedimentary Geology*, 26(1–3), 139–156.

Hein, C.J.; FitzGerald, D.M.; Carruthers, E.A.; Stone, B.D.; Barnhardt, W.A., and Gontz, A.M., 2012. Refining the model of barrier island formation along a paraglacial coast in the Gulf of Maine. *Marine Geology*, 307(April 2012), 40–57.

Jol, H.; Smith, D., and Meyers, R., 1996. Digital ground-penetrating radar (GPR): An improved and very effective geophysical tool for studying modern coastal barriers (examples for the Atlantic, Gulf and Pacific coasts, USA). *Journal of Coastal Research*, 12(4), 960–968.

Keay, D.L., 2001. A history of Washburn Island. *Bridgewater Review*, 20(2), 22–25.

Khalil, S.M.; Finkl, C.W., and Raynie, R.C., 2013. Development of new restoration strategies for Louisiana barrier island systems, northern Gulf of Mexico, USA. *In:* Conley, D.C.; Masselink, G.; Russel, P.E., and O'Hare, T.J. (eds.), *Proceedings of the 12th International Coastal Symposium*, Journal of Coastal Research, Special Issue No. 65, 1467–1472.

Little, E.A., 1993. Radiocarbon age calibration at archaeological sites of coastal Massachusetts and vicinity. *Journal of Archaeological Science,* 20(4), 457–471.

Ludlum, D.M., 1963. *Early American Hurricanes, 1492–1870,* 1st edition. Boston, Massachusetts: American Meteorological Society, 338p.

Mague, S.T., 2012. Retracing the past: Recovering 19th century benchmarks to measure shoreline change along the outer shore of Cape Cod, Massachusetts. *Cartography and Geographic Information Science*, 39(1), 30–47.

Maio, C.V.; Gontz, A.M.; Weidman, C.R., and Donnelly, J.P., 2014. Late Holocene marine transgression and the drowning of a coastal forest: Lessons from the past, Cape Cod, Massachusetts, USA. *Palaeogeography, Palaeoclimatology, Palaeoecology*, 393, 146–158.

Maio, C.V.; Tenenbaum, D.E.; Brown, C.J.; Mastone, V.T., and Gontz, A.M., 2012. Application of geographic information technologies to historical landscape reconstruction and military terrain analysis of an American Revolution Battlefield: Preservation potential of historic lands in urbanized settings, Boston, Massachusetts, USA. *Journal of Cultural Heritage*, 14(4), 317–331.

Mallinson, D.J.; Smith, C.W.; Culver, S.J.; Riggs, S.R., and Ames, D., 2010. Geological characteristics and spatial distribution of paleo-inlet channels beneath the Outer Banks barrier islands, North Carolina, USA. *Estuarine, Coastal and Shelf Science*, 88(2), 175–189.

Mallinson, D.J.; Smith, C.W.; Mahan, S.; Culver, S.J., and McDowell, K., 2011. Barrier island response to late Holocene climate events, North Carolina, USA. *Quaternary Research*, 76(1), 46–57.

MassGIS, 2013. *Office of Geographic Information (MassGIS).* http://www.mass.gov/anf/research-and-tech/it-serv-and-support/application-serv/office-of-geographic-information-massgis/.

McNinch, J.E., 2004. Geologic control in the nearshore: Shore-oblique sandbars and shoreline erosional hotspots, Mid-Atlantic Bight, USA. *Marine Geology*, 211(1), 121–141.

Miller, W.R. and Egler, F.E., 1950. Vegetation of the Wequetequock-Pawcatuck tidal-marshes, Connecticut. *Ecological Monographs*, 20(2), 143–172.

Murray, J.W., 2006. *Ecology and Applications of Benthic Foraminifera.* Cambridge, New York: Cambridge University Press, 440p.

NOSAMS (National Ocean Sciences Accelerator Mass Spectrometry Facility), 2014. *Sample Preparation,* http://www.whoi.edu/nosams/Sample_Prep.

Neal, A., 2004. Ground-penetrating radar and its use in sedimentology: Principles, problems and progress. *Earth-Science Reviews*, 66(3), 261–330.

Neal, A. and Roberts, C.L., 2000. Applications of ground-penetrating radar (GPR) to sedimentological, geomorphological and geoarchaeological studies in coastal environments. *Geological Society of London, Special Publications,* 175(1), 139–171.

Nicholls, R.J.; Wong, P.P.; Burkett, V.; Codignotto, J.; Hay, J.; McLean, R.; Ragoonaden, S., and Woodroffe, C.D., 2007. Coastal systems and low-lying areas. *In:* Parry, M.L.; Canziani, O.F.; Palutikof, P.J., and van Hanson, C.E. (eds.), *Climate Change 2007, Impacts, Adaptation and Vulnerability—Contribution of Working Group II to the Fourth Assessment Report of the Intergovernmental Panel on Climate Change*, Cambridge, U.K.: Cambridge University Press, 42p.

Niering, W.A.; Warren, R.S., and Weymouth, C.G., 1977. Our dynamic tidal marshes: Vegetation changes as revealed by peat analysis. *Connecticut Arboretum Bulletin,* 22, 1–12.

NOAA (National Oceanic and Atmospheric Administration), 2014. *Tides and Currents, Extreme Water Levels for Woods Hole, MA, SationID: 8447930.* http://tidesandcurrents.noaa.gov/est/est_station.shtml?stnid=8447930.

Oldale, R. and O'Hara, C., 1984. Glaciotectonic origin of the Massachusetts coastal end moraines and a fluctuating late Wisconsinan ice margin. *Geological Society of America Bulletin,* 95(1), 61–74.

Orson, R.A. and Howes, B.L., 1992. Salt marsh development studies at Waquoit Bay, Massachusetts: Influence of geomorphology on long-term plant community structure. *Estuarine, Coastal and Shelf Science*, 35(5), 453–471.

Reimer, P.; Baillie, M.G.; Bard, E.; Bayliss, A.; Beck, J.W.; Blackwell, P.G., and Edwards, R.L., 2009. IntCal09 and Marine09 radiocarbon age calibration curves, 0–50,000 years cal BP. *Radiocarbon*, 51(4), 1111–1150.

Roberts, M.L.; von Reden, K.F.; Burton, J.R.; McIntyre, C.P., and Beaupre, S.R., 2013. A gas-accepting ion source for accelerator mass spectrometry: Progress and applications. *Nuclear Instruments and Methods in Physics Research Section B: Beam Interactions with Materials and Atoms*, 294(January), 296–299.

Salzman, J., 1997. Valuing ecosystem services. *Ecology Law Quarterly*, 24(887), 1–18.

Scileppi, E. and Donnelly, J.P., 2007. Sedimentary evidence of hurricane strikes in western Long Island, New York. *Geochemistry, Geophysics, Geosystems*, 8(6), 1–25.

Scott, D. and Medioli, F., 1978. Vertical zonations of marsh foraminifera as accurate indicators of former sea-levels. *Nature*, 272(April), 528–531.

Seminack, C.T. and Buynevich, I.V., 2013. Sedimentological and geophysical signatures of a relict tidal inlet complex along a wave-dominated barrier: Assateague Island, Maryland. *Journal of Sedimentary Research*, 83(2), 132–144.

Stuiver, M. and Braziunas, T.F., 1993. Modeling atmospheric 14C influences and 14C ages of marine samples to 10 000 BC. *Radiocarbon,* 35(1), 137–189.

Turner, R.K.; Lorenzoni, I.; Beaumont, M.; Bateman, I.J.; Langford, I.H., and McDonald, A.L., 1998. Coastal management for sustainable development: Analysing environmental and socio-economic changes on the UK coast. *Geographical Journal*, 164(3), 269–281.

Uchupi, E. and Mulligan, A.E., 2006. Late Pleistocene stratigraphy of Upper Cape Cod and Nantucket Sound, Massachusetts. *Marine Geology*, 227(1), 93–118.

van Heteren, S.; FitzGerald, D.M.; Barber, D.C.; Kelley, J.T., and Belknap, D.F., 1996. Volumetric analysis of a New England barrier system using ground-penetrating-radar and coring techniques. *The Journal of Geology*, 104(4), 471–483.

van Heteren, S.; FitzGerald, D.M.; McKinlay, P.A., and Buynevich, I.V., 1998. Radar facies of paraglacial barrier systems: Coastal New England, USA. *Sedimentology*, 45(1): 181–200.

Williams, J.; Penland, S., and Sallenger, A.H., Jr. (eds.), 1992. *Louisiana Barrier Island Erosion Study: Atlas of Shoreline Changes in Louisiana from 1853 to 1995*. Denver, Colorado: U.S. Geological Survey, *Miscellaneous Investigations Series I-2150-A*.